6 Discussion and conclusions

In this chapter the most general effects induced by intercalation, which have been observed by photoelectron spectroscopy, will be summarized and discussed. This will be done by comparing the chemical shifts observed in the core-level emission lines with variations in the valence band spectra. A correlation with charge transfer induced by intercalation will be attempted. It will be shown to what extent measurable modifications of the electronic structure from the pure host to the intercalation compound can account for the energetic gain of the intercalation reaction.

6.1 Binding energy shifts and charge transfer

A precise evaluation of the experimentally determined binding energies for its core-level emission lines and of the observed changes in the valence band spectra is often not easy. Nevertheless the whole set of intercalation experiments performed during this work gives some general trends.

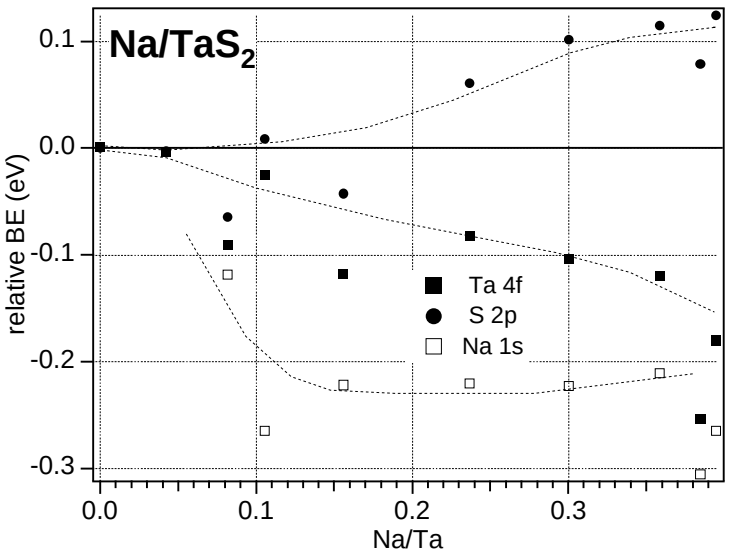

Fig. 6.1 Relative binding energy shifts for the Ta 4f, S 2p and Na 1s core-levels lines after deposition steps of increasing Na amounts on 1T-TaS_2. BEs have been deduced after 1-component fit of the core levels. The lines are given as a guide to the eye

Fig. 6.1 shows a typical BE evolution of the core levels during Na deposition on 1T-TaS_2. The shifts of the reference level (the position of E_F vs. E_{vac}) is clearly indicated by similar shifts at specific deposition steps. Such variations of the reference are mainly due to the transformation of the valence band structure induced by Na intercalation. In spite of this dependence the different core levels show in addition distinct and different tendencies in dependence of the intercalated Na. The chalcogen peak tends to shift to higher BE whereas the transition metal tends to shift to lower BE. For the latter, the determination is complicated by the probable presence of a low-BE chemically shifted component. The BE of the intercalate (guest species) was even more difficult to establish, because besides the possible presence of a surface Na component at higher BE the peak was very

weak at the early deposition stages. A tendency of chemical shifts closer to that of the transition metal can however be noticed.

Similar trends have been observed for all investigated systems with large positive binding energy shifts of the chalcogenide and small often negative binding energy shifts of the transition metal. Since it is possible to distinguish qualitatively the effects of the displacement of the reference level $E_F^{vac}(x)$ from changes in the atoms' environment ($BE_{CL}(x)$), some conclusions on the charge transfer may be attempted.

Considering the core level CL of an atom in the intercalation compound, we may split the energy relative to the vacuum as a function of the alkali concentration x in dependence of both the position of the Fermi level and of its variation due to the host-guest interaction:

$$E_{CL}^{vac}(x) = E_F^{vac}(x) - BE_{CL}(x) = E_{CL}^{vac}(0) - \Delta BE(\alpha \cdot \gamma_{CL}, x) \qquad \textit{(Eq. 6.1)},$$

where α is the fraction of electron transferred to the considered atom per each alkali, and γ_{CL} is its screening effect on the core level CL (this depends on the Slater's screening coefficient of the valence states on the core level [275, 276]). ΔBE a monotonic function of its variables ($\alpha \cdot \gamma_{CL}$ and x), its value is 0 when either variable is 0. Due to intercalation there is first of all a variation of the position of the Fermi level due to the filling of conduction band states, which affects $E_F^{vac}(x) = E^{vac} - E_F(x)$. As a consequence variations of the position of the Fermi level affect all BEs. In addition evolutions with x are specific of the atomic species in the intercalated compound, as $\alpha\gamma_{CL}$ is specific for each atom and $\Delta BE(\alpha \cdot \gamma_{CL}, x)$ shifts differently for the different core lines. The observed tendencies indicate that $\alpha\gamma_{CL}$ is larger for the transition metal than for the chalcogen. Thus, for TiS_2 γ_{Ti2p} may be assumed not greater than γ_{S2p}. This means that α, i.e. the charge transfer is larger to the transition metal than to the chalcogen, as expected. For Na the only possible comparison is between the cases of diluted or concentrated intercalate. The development clearly diverges from S 2p. This indicates a growing screening of Na, surprisingly nearly as much as the transition metal. This may be possibly justified by a high γ_{Na1s}, but requires that part of the charge remains localized to the Na 3s level. As a consequence it has to be deduced that intercalated Na does not completely donate its electron to the host species forming a Na^+ ion but has to be included into the overall change in electronic structure.

A similar diagram applied to the thin film TiS_2 electrochemical cell is shown in Fig. 6.2, where also the variation of the Cl 2p line is reported. In the case of Cl 2p α is evidently zero and the evolution should reflect only the shifts of the Fermi level. The large shift of the Fermi level contradicts a prediction given by McKinnon. According to McKinnon [75, 76, 105, 272] the value $E_F^{vac}(x)$ should not be affected by drastic variations in the rigid band model. This statement is based

on theories developed to explain the electronic structure of metal alloys [71]. The field of the intercalated alkali ion is screened by the donated free electron over some distance L. Since in a metal this distance is comparable with the host's interatomic distances, there will be regions of the solid where no extra electrons are present. In such regions the Fermi energy will remain locally constant. But the Fermi level is the same all over the equilibrated electronic conductor. Thus, if the Fermi level is constant at some point of the solid, it must remain constant at any point. This is possible because the bands are locally pulled down by the alkali ion's electric field. Although electrons are donated to the hosts' conduction band, they will remain localized in regions where the band energy decrease balances the occupancy of higher electronic levels. The failure of McKinnon's prediction can be understood if the screening length L in the intercalation compound Na_xTiS_2 is larger than in metals.

The large difference between the shift of Cl 2p and S 2p demonstrates that part of the electronic charge is also transferred from Na to S. The charge transfer to S agrees with recent literature [82, 83, 273, 274], and can be explained by considering the important covalent component of the Ti-S bond in TiS_2 (see also §2.1.2). Thus, based on the BE shifts it may be concluded that charge is transferred mainly to Ti, but in part also to S, and a residual should remain localized on the intercalated Na. The experimentally observed tendencies in the BEs for Na 1s indicated by the diagram of Fig. 6.2 suggest also an increased localization of the donated electron around the Na ions. It should be noted that a charge transfer to S cannot be identified in any new component in the S 2p signal, as it should be expected with a contribution at low BE.

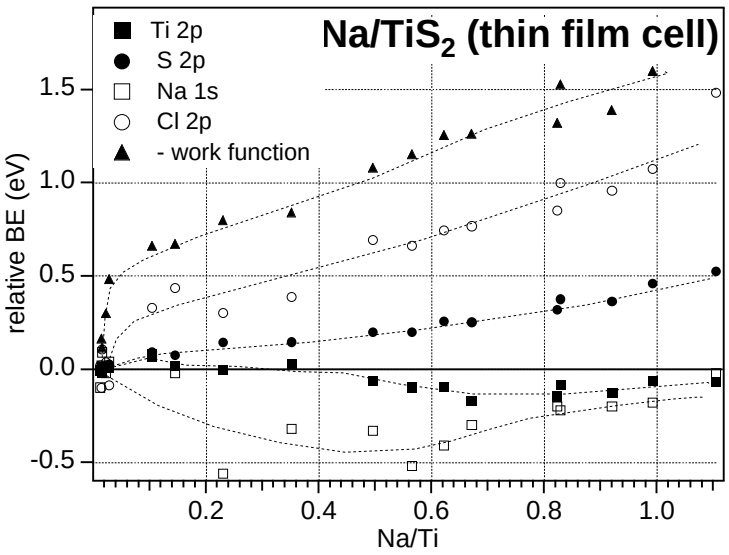

Fig. 6.2 Relative binding energy shifts for the Ti 2p, S 2p, Na 1s and Cl 2p core-levels lines after electrochemical intercalation of increasing Na amounts on a TiS_2 thin film. BEs have been deduced after 1-component fit of the core levels. The variation of work function, changed of sign for consistency, is also reported. The lines are given as a guide to the eye

It should be emphasized that the shift of the different S levels, referred to the Fermi level, is not the same. The shift of the S 2p core-level line during the whole Na/TiS_2 experiment was about 0.5 eV. In comparison the S 3p valence band states shifted much more: the main peak (D) of the

spectra reported in Chapter 5 shifts by over 1 eV (relative to E_F). As already discussed before in relation to the He I spectra, several effects can account for the shift in the valence band S 3p states without involving screening effects. With non-stoichiometric samples the Fermi level is pinned at the bottom of the Ti 3d t_{2g} states. In an absolute energy scale e.g. vs. E_{vac} the expansion of the van der Waals gap and the loss of electronic coupling of the layers leads to a shift of Ti 3d levels to higher energy and of the S 3p levels to lower energy (opening of a gap). In contrast the S core lines would not be changed in energy in the absolute scale. If, however, E_F is chosen as a reference as in photoemission experiments both lines will shift, but the valence band S 3p states will be shifted more. The idea of a sample less intercalated in the bulk observed with different signal surface sensitivity (UPS vs. XPS) can be ruled out, because the S 2p signal do not show a relevant component at higher BE. But an alternative and possibly also valid explanation is the different Slater's electron-screening coefficient [275, 276] of the extra valence electron for the different states. The different shifts would then confirm that a partial electron transfer takes place also to the valence levels of S, which will lead to better hole screening than for the deeper S 2p states. The different shifts of the components in the Ti 2p peak cannot be easily interpreted. Possibly the defective Ti acts as a trap for the injected electrons, while the remaining Ti has an electron screening comparable to that of S.

As for S in Na/TiS_2 the Se 3d BEs in $Na/TiSe_2$ are found to increase less than the valence band states, with shifts of 0.25 eV and 0.4 eV, respectively. This occurs even though the s/p band gap opening does not take place in this system. It may indicate a covalent interaction between the chalcogen and the host ions with stabilization of the chalcogen valence orbitals. It can be recalled that Umrigar *et al.* found with their self-consistent band calculation a higher electronic density in planes between Li and S than between S and Ti [43]. With more recent methods Kim *et al.* found for $LiTiX_2$ an overlap electron population of 0.35 (0.37) for the Ti-S (Ti-Se) bond and 0.173 (0.176) for the Li-S (Li-Se) bond.

These effects in the valence band are clear deviations from the rigid band model, and give further elements to explain why McKinnon prediction fails in the systems investigated here. In particular the opening of the van der Waals gap (with subsequent decoupling of the inter-layer covalent interaction) combined with the specific Na-X interaction (much stronger than Na-Ti) should increase the energy of the Ti 3d levels in the absolute scale and thus also of the Fermi level.

6.2 The ionic and electronic contributions to the electrochemical potential

The above given discussion of the different effects, which simultaneously affect the core level and valence state BEs with intercalation clearly indicate that it is no easy task to deduce the

shift of $E_F^{vac}(x)$ which should be related to the chemical potential of electrons with intercalation. Fortunately the experiments with the thin films of TiS_2 can be evaluated in this sense as an inert probe (Cl from the deposition sequence) was present in the sample. The chemical environment of Cl is expected to remain unchanged during the intercalation-deintercalation cycles. If the contact potential between TiS_2 and NaCl contamination phases can be considered constant too, we have an internal probe for the variation of the chemical potential of the electrons. As shown in Fig. 2.8 the electronic chemical potential μ_e corresponds to the difference between the Galvani (inner) potential and the Fermi level. If the contact potential between TiS_2 and the Cl-containing phase is constant, all Cl electronic levels will not to shift with respect to the Galvani potential in TiS_2. Thus it can be written

$$BE_{Cl\,2p} - \mu_e = const \qquad \textit{(Eq. 6.2).}$$

The other probe, the work function, should also reflect changes in the position of $E_F^{vac}(x)$ in the bulk but may be affected by surface dipoles due to adatoms. In fact, the relationship between work function and electronic chemical potential depends also on the surface potential χ:

$$\mu_e = e\chi - \Phi \qquad \textit{(Eq. 6.3).}$$

The effect of the surface dipole is shown in Fig. 6.2, where also the variation of work function (with changed sign) is reported. For small Na contents, when most of the surface dipole are formed, the work function has a clear drop of 0.5 V, whereas the corresponding decrease of the Cl 2p BE is much smaller. After this initial drop the work function has a slope which is only slightly higher than the Cl 2p BE, possibly related to further dipole formation. Apart of the surface dipole, which can be well recognized, the two measurements of the variation of the chemical potential of the electrons are consistent. This allows the estimation of the relative contributions of the electronic and ionic chemical potentials to the battery voltage, according to §2.2.4. However, for the reason just explained not Eq. 2.15, based on the work function, will be considered, but its corresponding equation based on the binding energy shift of the Cl 2p level:

$$e\frac{d}{dx}V = -\frac{d}{dx}BE - \frac{d}{dx}\mu_{A^+} \qquad \textit{(Eq. 6.4).}$$

The TiS_2 potential as function of the charge could be measured on the same cell used in UHV experiments later in the glove box, using a 3-electrode configuration where metallic Na was applied for both reference and counter electrodes. The voltage/charge profile for a charge-discharge cycle is reported in Fig. 6.3. As in the 2-electrode configuration in UHV, the curve does not exhibit evident steps, which are related to stacking transitions. Additionally, compared with the literature [268-270] the voltage drops to much lower values. A possible explanation can be the less

monodisperse composition. The large amount of self-intercalated Ti is possibly also occupying favorable intercalation sites, decreasing considerably the free energy of intercalation. On the same energy scale of the cell voltage the variations of Cl 2p BE are reported. Initially the rapid fall of the voltage corresponds to a fall of the electronic chemical potential. This is possibly due to the relatively low density of the empty states immediately above the Fermi level. It can be seen that the voltage decreases more rapidly than the line formed by the BE values measured with PES. This proves that the variation of the voltage cannot be associated only to the chemical potential of the electrons, since also the chemical potential of the ions decreases. Nevertheless, the electronic component proves to contribute for about 60% of the battery voltage.

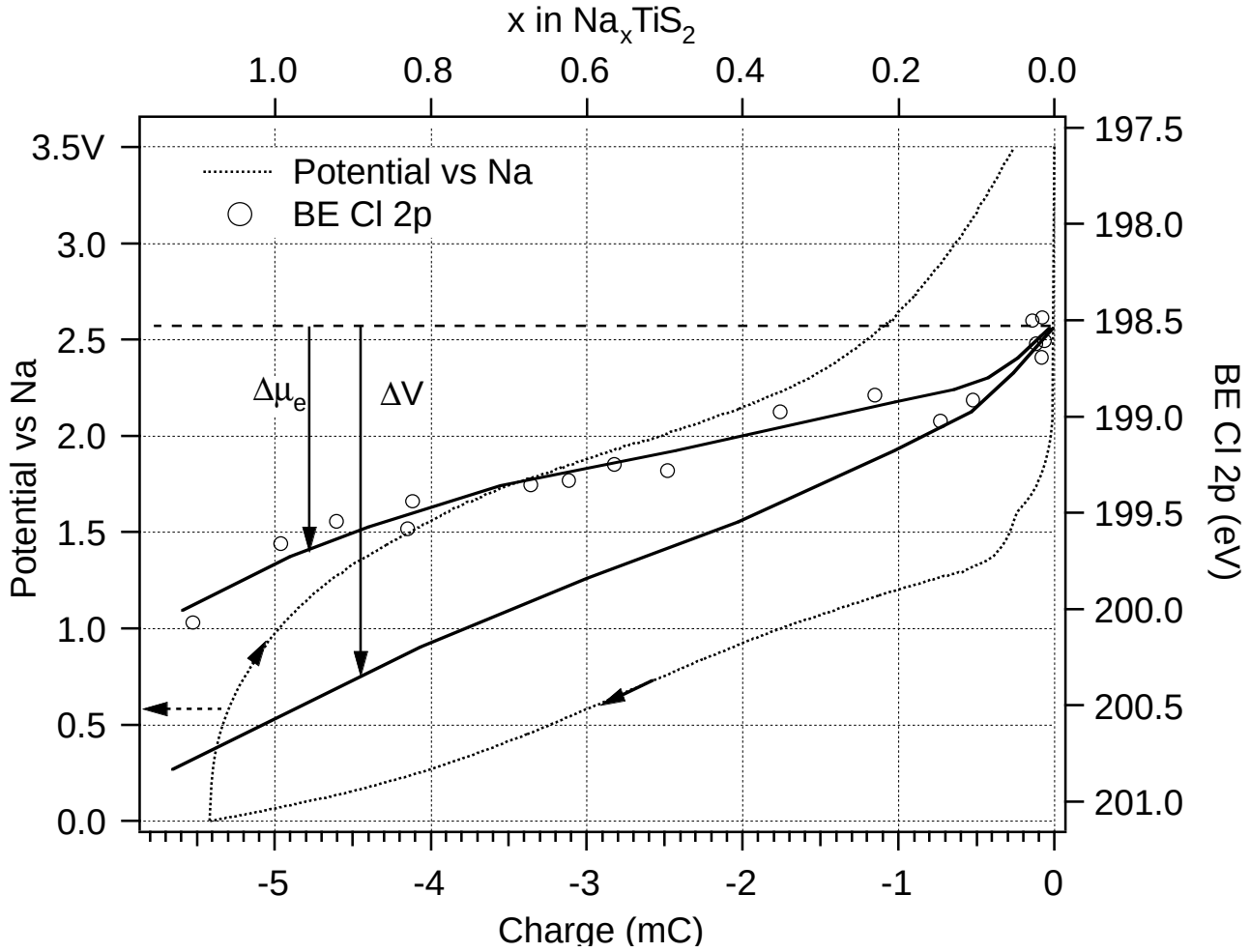

Fig. 6.3 The variation of the electrochemical potential and of the chemical potential of the electrons in a TiS_2 thin film cathode as function of the intercalated Na content. The electrochemical potential is deduced from the voltage in a 3-electrode cell, and the chemical potential of the electrons from the Cl 2p binding energy shift. The lines are given as a guide to the eye, and are approximately deduced from the average values of voltage or binding energy. Note that the arrows have the same orientation due to the opposite scale of the left and right axis

This distinction has a physical meaning only in the frame of the rigid band model. A strong correlation between inserted cations and electrons, such as the formation of partial Na-S covalent

bonding interaction seems to be confirmed by the chemical shift of the Na signals. This would imply on one hand that the electronic levels depend on the specific (chemical) interaction with $Na^{\delta+}$, and on the other that the activity of $Na^{\delta+}$ does not depend only on its concentration and on the electrostatic interactions.

6.3 Summary of results and perspectives

The experiments of alkali deposition on single crystals have shown how samples prepared with this process do not equilibrate although they can be readily intercalated. Material parameters like the presence of defects or the amount of self-intercalated Ti influences the kinetics of the alkali distribution in the obtained intercalated material.

The preparation of a polycrystalline thin film provided a host, where the diffusion barrier to equilibrium concentration distributions could be easily overcome in the deposition experiment performed at RT.

The direct preparation of the thin film on a solid electrolyte allowed the *in-situ* preparation of an electrochemical cell, a device that could be used for the finest reversible control of the intercalated doses. This also allowed for the first time to simultaneously measure the electronic structure of the intercalation compound and the voltage of the cell where it is used as electrode. This measurement provides the parameters for the quantitative correlation of the electrode potential profile with the energy of the available host's sites for the electrons. Thus, the estimation of the relative contributions of the site energy for ions and electrons to the battery voltage was achieved. This is the same as saying that it was possible to obtain experimentally a quantitative correlation between the electronic structure and the thermodynamic values. For the prepared TiS_2 thin film it has been found that variation of the chemical potential of the electrons contribute to about 60% of the voltage drop of its Na intercalation battery. Consequently, in this system rigid band assumptions, which consider the ionic contribution relatively constant and relate features in the voltage vs. composition curve to the electronic structure of the host, can be considered valid as only a first rough approximation. This confirms the important role of the detailed knowledge of the electronic structure of the intercalation compound to understand and predicts this important parameter of a battery performance. With the techniques applied in this work changes of the electronic structure could be carefully followed and related to the guest concentration. The limits of the rigid band model in the investigated systems could be set. In TiS_2 an evident opening of a gap between the S 3p and the Ti 3d bands was found. In the related host $TiSe_2$ a corresponding effect between Se 4p and Ti 3d was not observed. This indicates that the extent of the validity of the rigid band model is very sensitive to the specific material considered. The electronic hybridization suggested by the collected data indicates that the classic picture assuming that the alkali outer shell

electron is completely donated to reduce the transition metal center is too much simplifying. Although it is true that most of the charge resides close to the transition metal, an important part is also transferred to the chalcogen.

Electron coupling and delocalization can be evaluated only by the systematic comparison of different host materials. TMDCs would provide a class of structurally similar and electronically different materials. The degree of localization could be evaluated with more ionic compounds such as the oxides. Using crystals (i.e. accessing only a limited guest concentration range) useful comparisons could be only partially obtained in the present work. It is to expect that thin films of a broader choice of hosts would provide more general information.

Also the measurement technique using the thin film cathode may be improved. A rather obvious improvement of the experimental setup as used so far is to find a reliable reference electrode for the simultaneous measurement of potential and electronic structure without a second measurement in the glove-box. A possibility is to use compounds whose electrochemical potential is higher than the reduction of water. Na-oxychlorides such as $Na_xWO_2Cl_2$ satisfy this requirement, having a discharge curve lying above 2.7 V vs. Na [277]. Na intercalation compounds of layered oxides are not well-studied, but may also have a high potential and thus represent a possible choice for a layer to use as both reference and counter electrode. Such materials should be stable also at the synthesis conditions of the thin film cathode. Alkalis in metallic form have a too low vapor pressure, and cannot be proposed for UHV operation. However, in a 3-electrode configuration the current flow in the reference is negligible. For this reason in electrochemical experiments often a pseudoreference is used, which is typically an inert metallic conductor, in contact with the electrolyte. For instance graphite in contact with the Na-β''Al_2O_3 electrolyte has a typical potential vs. Na of about 2.7 V. Two electrically isolated graphite layers can thus be used as reference and counter electrode, respectively. With appropriate modification to the sample carriers it should be possible to obtain measurements in a 3-electrode configuration directly in UHV.

The same experiment may be easily extended to materials of more current interest than dichalcogenides. Some preparations of intercalated oxides at low pressure have already been reported [119, 278-281]. For the direct investigation of Li intercalation synchrotron radiation is important to reach a high cross section of the Li 1s line.

The most interesting applications would be possible if the same electrode material prepared ex-situ for batteries could be investigated in UHV. Some attempts to analyze intercalation materials with PES have been reported in the literature [103, 104], and it has been shown that after proper sample treatment even details in UP spectra could be well resolved. The requirement of an extremely thin electrode is only related to the time needed to intercalate and equilibrate the

intercalation electrode to measure. In principle polymeric electrolytes should provide higher conductivity than Na-β''alumina and may still be suitable for UHV operation. It is thus realistic to envisage such experiments as that reported in this work directly to common laboratory-prepared solid-state intercalation batteries.